Hindawi
Adsorption Science & Technology
Volume 2021, Article ID 5728696, 12 pages
https://doi.org/10.1155/2021/5728696

Research Article

Elimination of Congo Red Dye from Industrial Wastewater Using *Teucrium polium L.* as a Low-Cost Local Adsorbent

Nasser A. Alamrani and Hatem A. AL-Aoh

Department of Chemistry, Faculty of Science, University of Tabuk, 71474 Tabuk, Saudi Arabia

Correspondence should be addressed to Hatem A. AL-Aoh; halawah@ut.edu.sa

Received 19 May 2021; Revised 18 June 2021; Accepted 25 June 2021; Published 14 July 2021

Academic Editor: George Kyzas

A novel adsorbent prepared from the leaf powder of *Teucrium polium L.* (TPLLP) was characterized and its ability for adsorption of Cong red (CR) was inspected. Influences of CR concentration, adsorbent dosage, time of agitation, pH of solution, and temperature on the performance of this adsorption were also examined. Three models of kinetic along with three different isotherm models were applied for analyzing the empirical data of this adsorption. Additionally, the thermodynamic constants of were decided. The surface area, pore volume, pore size, and pH_{ZPC} of Zn/Cu-TPLLP were found to be 2.6436 $m^2.g^{-1}$, 0.013317 $cm^3.g^{-1}$, 527.393 Å, and 8.8, respectively. The achieved outcomes indicate the positive influence of temperature, concentration of CR in the range of 20 to 900 mg/L, adsorbent mass in the range of 0.005 to 0.02 g, time of adsorption from 0 to 120 min, and pH from 5.5 to 8.5. Models of the 2nd order with $R^2 \geq 0.995$ and Langmuir with $R^2 \geq 0.990$ were the best among the other kinetic and isotherm models applied in this research. Moreover, superior capacities of 526.32, 666.67, and 909.09 ($mg.g^{-1}$) were stemmed at 27, 42, and 57°C, respectively. The outcomes of the thermodynamic evidenced that this adsorption is spontaneous and a heat absorber.

1. Introduction

The dye of Congo red (CR) is known as typically anionic diazo dye having four different color-assisted functional groups [1], which has an IUPAC name of disodium 4-amino-3-[4-[4-(1-amino-4-sulfonato-naphthalen-2-yl) diazenylphenyl] phenyl] diazenyl-naphthalene-1-sulfonate [2] and has various molecular structures in the aqueous solutions that differ in their pH [2]; it is highly soluble in water and stable in air and light [3]. CR dye is used in laboratories as a pH indicator, histological dye, amyloidosis diagnosis, and for testing the contents of HCl in gastric [3]. This dye is also used in various industries like industry of textile due to its significant affinity to fibers of cellulose, papermaking, and industry of plastic, cosmetics, and pharmaceuticals [4, 5]. CR is a member of benzene compounds and contains in its structure aromatic amines; therefore, it will be converted to carcinogenic materials in the environment [3, 6]. Moreover, benzidine produced from metabolizing of CR poses hazard effects on human health such as irritation of gastrointestinal, eye, and skin [3]. Benzidine also causes clotting of blood, somnolence, and breathing problems [3]. Consequently, it is necessary to remove CR from sewage of those laboratories and industries before their discharge to the aquatic system. Thus, conventional biological methods have been established for decolorization of CR from the sewages of laboratories and industries, e.g., fungi of white rot [7], and foams of polyurethane and polypropylene [8] were applied for biodegradation of CR. It was reported that the biodegradation efficiency of CR is insufficient due to different aromatic structures and synthetic origin of this dye [9]. Therefore, other traditional techniques like electrocoagulation [10], coagulation by Fe_3O_4 [11], membrane filtration [12], and precipitation by chemical agents [13] were also utilized for removing of CR from water. The high cost and low removing performances of these methods prove that their usage is ineffective. Photocatalytic degradation of CR by activated hydrotalcites [14], cobalt ferrite nanostructures [15], nickel oxide nanoparticles [16], $CuS-Bi_2Cu_xW_{1-x}O_{6-2x}$ nanocomposite [17], and zinc oxide nanoparticles [18] was

also investigated. Despite the effectiveness of the photocatalytic degradation techniques towards CR, the harmfulness of this dye may be less than that of its degradation products.

Additionally, various sorbents such as activated carbon prepared from different materials [19–21], different clays [22] carbon loaded by nanoparticles of cobalt [23], magnetic nanocomposites of Co_3O_4 and SiO_2 [24], binary oxide of iron zirconium [25], nanoparticles of MgO [26], and nanoparticles of SnO_2 [27] were used to purify the sewages from CR. In comparison with other methods, the adsorption of CR by these adsorbents was found to be the best in terms of its efficiency, easy design, and operation [28]. Therefore, adsorption was selected in this study as the standard technique for removing of CR from synthetic aqueous solutions.

Although the nanoparticles of metallic oxides and activated carbon have a high adsorptive performance, their usages become limited due to the high costs of their production. Hence, several low or uncostly materials were applied as effective adsorbents for CR elimination from waters, e.g., hydrothermal-treated mushroom [1], powder of shrimp shell [2], tea waste [29], bottom ash and de oiled soya [3], and conjugates of sodium alginate-*Chlorella* polypyrrole-*Chlorella*[30]. The outcomes of these studies indicate that there are big differences between the adsorption performances of these cheap adsorbents towards CR. Therefore, other works should be carried out to investigate CR adsorption by other low-cost sorbents.

Teucrium polium L. (TPL) or germander is a herbal plant that has been utilized for more than 2000 years as traditional herbal remedies for their antifungal, carminative, antispasmodic, antipyretic, anti-inflammatory activity, and their ability to decrease high blood pressure [31]. This herbal plant belongs to *Lamiaceae* family that contains around 300 species and the flowering time of these herbs is between June and August. These species are abundantly distributed on hills and mountains in different locations such as Mediterranean countries, Southwest Asia, North Africa, and Europe [31, 32]. This plant is rich in flavonoids and commonly known in Saudi Arabia as Ja'adeh [32].

In the case of wastewater treatment, TPL has been used previously for preparation of Fe_2O_3 nanoparticles, which are used as a catalyst for photodegradation of methyl orange dye [33] and as an adsorbent for arsenic (III) removal from the aqueous solutions [34].

Despite the cheapness of this herbal plant and its availability in a considerable amount in many different countries, especially in Tabuk City and others in Saudi Arabia, there is no attempt that has been carried out till now to use the *Teucrium polium L.* leaf powder (TPLLP) as a new adsorbent for the removal of hazardous dyes from water or wastewater. Therefore, the main object of this work is to evaluate the adsorption efficiency of CR by using TPLLP as a novel, available, and cheap adsorbent. To achieve this aim, the leaf powder of this herb was modified by copper sulfide, zinc chloride ($ZnCl_2$), and oxalic acid (HO_2CCO_2H); the modified and unmodified samples were characterized and the adsorptive performances of CR by these adsorbents were compared to select the best one. After that, influence of experimental conditions along with constants of kinetics, isotherms, and thermodynamic was examined for adsorption of CR by the best adsorbent prepared and tested in this work.

2. Materials and Methodology

2.1. Materials and Chemical Agents. The leaves of *Teucrium polium L.* (TPL) were supplied by a market located in Tabuk City, Saudi Arabia. Chemical reagents such as hydrochloric acid HCl (37%), sodium hydroxide NaOH with purity ≥ 97 % $ZnCl_2$ with purity ≥ 97%, HO_2CCO_2H with purity ≥ 99.99%, CuS with purity ≥ 99.99%, and Na_2CO_3 with purity ≥ 99.00% were obtained from Sigma-Aldrich and used in this research.

2.2. Modification of TPLLP. The leaves of TPL were twice washed by distilled water, dried in an oven, and then converted to powder by electric grinder (TPLLP). A 100 g of TPLLP was refluxed with 1 L of 20% *w*/*w* of $ZnCl_2$ at the boiling point for 180 min, and after this time, the mixture was left at room temperature for cooling. The cooled mixture was filtered and the remaining solid was heated with 250 mL of 2 M HCl for 90 min to remove the excess amount of $ZnCl_2$. Then, the solid part of the new mixture was disconnected by filtration and repeatedly rinsed by distilled water. Then, the clean solid was put for 30 h in an oven at 130°C for dehydration. Finally, the dehydrated solid was grinded, sieved to get homogeneous particles, and labeled as Zn-TPLLP.

Similar conditions and processes were applied for the mixture consisting of 100 g TPLLP and 50 g of CuS. The resulted adsorbent in this case was labeled as Zn/Cu-TPLLP.

A 100 g of TPLLP was also refluxed with 1 L of 20% *w*/*w* oxalic acid solution by applying the same experimental conditions and procedures mentioned above. The resulted sample was named as Ox-TPLLP.

2.3. Characterization of Adsorbents. At a 10 kV accelerating voltage, the modified and unmodified TPLLP samples were scanned by SEM equipment to identify the surface morphology of these adsorbents. These adsorbents were also scanned by the instrument of FT-IR (Nicolet iS5 of Thermo Scientific FT-IR, USA) to detect the types of the functional groups on the surface of these samples.

The technology of BET (NOVA-2200 Ver. 6.11) was applied at 77.35 K for 22 h to estimate the surface area and porosity of these adsorbents. Furthermore, five solutions of 0.05 M Na_2CO_3 with different initial values of pH (2, 4, 6, 8, and 10) (pH_i) were prepared. 40 mL of each solution was mixed with 0.2 g of the ideal adsorbent in a 150 mL plastic bottle. The bottles were shaken in shaker incubators at 27°C and 175 rpm for 26 h. Then, each solution was separated by filtration and the final pH (pH_f) of each one of these five solutions was measured using a pH meter. Finally, the values of (pH_i – pH_f) were computed and plotted against the values of pH_i to assess the pH_{ZPC} value of this adsorbent.

2.4. Adsorption Experiments

2.4.1. Determination of the Ideal Adsorbent. To identify the best and the most effective adsorbent prepared in this work towards CR, 20 mL of 100 mg/L CR solution was mixed with

Table 1: Summary of the empirical conditions for adsorption of Congo red by Zn/Cu-TPLLP.

Experiment type	Concentration of CR ($mg.L^{-1}$)	Adsorption time (min)	Adsorbent dosage (g)	pH	Temperature (°C)
Influence of dosage	60	1320	0.005-0.035	7	27
Influence of time	60, 150, 300	0-420	0.02	7	27
Influence of pH	300	1320	0.02	5.5-11.5	27
Influence of temp and CR conc.	300	1320	0.02	7	27-25

q_t and q_e ($mg.g^{-1}$): amount of CR adsorbed at time t and equilibrium (min), K_1 (1/min), and K_2 ($g.mg^{-1}.min^{-1}$) rate constants of the kinetic models for the 1st and 2nd orders, correspondingly. K_{dif} ($mg.g^{-1}.min^{-1}$)1/2: intraparticle diffusion rate constants. C: another kinetic constant.

Table 2: Kinetic models applied in this work.

Kinetic model	Linear equation	Plot	Parameters
Pseudo 1st order	$\log(q_e - q_t) = \log(q_e) - K_1 \frac{t}{2.303}$	$\log(q_e - q_t)$ vs.t	$k_1 = -\text{slope}$ $q_e = \exp(\text{intercept})$
Pseudo 2nd order	$\frac{t}{q_t} = \frac{1}{K_2(q_e)^2} + \frac{t}{q_e}$	$\frac{t}{q_t}$ vs.t	$k_2 = \frac{(\text{slope})^2}{\text{intercept}}$ $q_e = (\text{slope})^{-1}$
Intraparticle diffusion	$q_t = K_{dif}\sqrt{t} + C$	q_t vs. $\sqrt{t}$	$K_{dif} = \text{slope}$ $C = \text{intercept}$

q_t and q_e ($mg.g^{-1}$): amount of CR adsorbed at time t and equilibrium (min), K_1 (1/min), and K_2 ($g.mg^{-1}.min^{-1}$) rate constants of the kinetic models for the 1st and 2nd orders, correspondingly. Kdif ($mg.g^{-1}.min^{-1}$)1/2: intraparticle diffusion rate constants. C: another kinetic constant.

0.03 g of raw leaf powder of TPL (TPLLP) in a 30 mL amber bottle. The sealed amber bottle was agitated by a shaker incubator for 30 h at 180 rpm and 27°C. Then, the mixture was filtered and the Jenway UV-6800 UV-Vis spectrophotometer was applied for measuring the balance concentration of CR in the filtrate at 500 nm. Similar experiments were carried out for the adsorption of this dye by the other three adsorbents (Zn-TPLLP, Zn/Cu-TPLLP, and Ox-TPLLP). Equations (1) and (2) were used for computing the CR percentage removal and amounts of CR adsorbed at equilibrium (q_e, $mg.g^{-1}$) by each of these adsorbents.

$$\%R = \frac{(C_\circ - C_e)}{C_\circ} \times 100, \quad (1)$$

$$q_e = \frac{V}{m}(C_\circ - C_e), \quad (2)$$

where $C_\circ$ and $C_\circ$ are the initial and final concentrations of CR solution, respectively.

2.4.2. Influence of Experimental Conditions. The experiments of CR adsorption by the ideal adsorbent (Zn/Cu-TPLLP) were achieved in a batch system to examine the influence of the most important factors like Zn/Cu-TPLLP dosage (0.005-0.035 g), contact time (0-420 min), and pH (5.5-11.5) as the CR solution color will be changed to blue at pH less than 5, CR concentration (20-1000 $mg.L^{-1}$), and temperature (27-57°C) on the adsorption. All of these experiments were carried out by mixing 20 mL of CR solution with the required amount of Zn/Cu-TPLLP in amber bottles (30 mL). Then, the sealed amber bottles were shaken at 180 rpm in a shaker incubator. After the required time for each experiment, the suspensions were filtered and the remaining CR concentrations were measured as mentioned in Section 2.2. The experimental conditions applied in this work are listed in Table 1.

Equations (2) and (3) are used for the calculation of the amount of CR adsorbed at equilibrium (q_e, $mg.g^{-1}$) and time t (q_t, $mg.g^{-1}$), respectively.

$$q_t = \frac{V}{m}(C_\circ - C_t), \quad (3)$$

where Ct is the CR concentration (mg.L-1) at contact time t. m is the mass of Zn/Cu-TPLLP (g), and V is the volume of CR solution (L).

2.4.3. Kinetic Studies. The experimental results of Section 2.3 for adsorption of 60, 150, and 300 $mg.L^{-1}$ of CR solutions by Zn/Cu-TPLLP at 27°C and various times (0-420 min) were analyzed by the linear forms of three different kinetic models (Table 2) to determine the parameters of these models. Then, the obtained kinetic data were used for the investigation of the rate and mechanism of this adsorption.

2.4.4. Isotherm Studies. The experimental data of Section 2.3 for adsorption of 20-1000 mg/L CR solutions by Zn/Cu-TPLLP (0.02 g) at a contact time of 22 h and various temperatures (27, 42, and 57°C) were analyzed by the linear equations of Langmuir, Temkin, and Freundlich isotherm models (Table 3) to evaluate the performance of this adsorption and to characterize the surface of Zn/Cu-TPLLP.

Table 3: Isotherm models used in this work.

Model name	Linear form	Plot	Constants
Langmuir isotherm	$C_e/q_e = (1/q_{\max}KL) + (C_e/q_{\max})$	(C_e/q_e) vs.C_e	$q_{\max} = (\text{slope})^{-1}$ $K_L = \dfrac{\text{slope}}{\text{intercept}}$
Freundlich isotherm	$\ln(q_e) = \ln(K_F) + \dfrac{1}{n}\ln(C_e)$	$\ln(q_e)$ vs.$\ln(C_e)$	$K_F = \exp(\text{intercept})$ $n = (\text{slope})^{-1}$
Temkin isotherm	$q_e = B_1 \ln(K_T) + B_1 \ln(C_e)$	q_e vs.$\ln(C_e)$	$B_1 = \text{slope}$ $K_T = \exp\left(\dfrac{\text{intercept}}{\text{slope}}\right)$

$q_{\max}$ (mg/g): maximum adsorption capacity. K_T, K_F, and K_L: constants of Temkin, Freundlich, and Langmuir, respectively. n: constants associated with intensity of adsorption. B_1: constants associated with the adsorption heat.

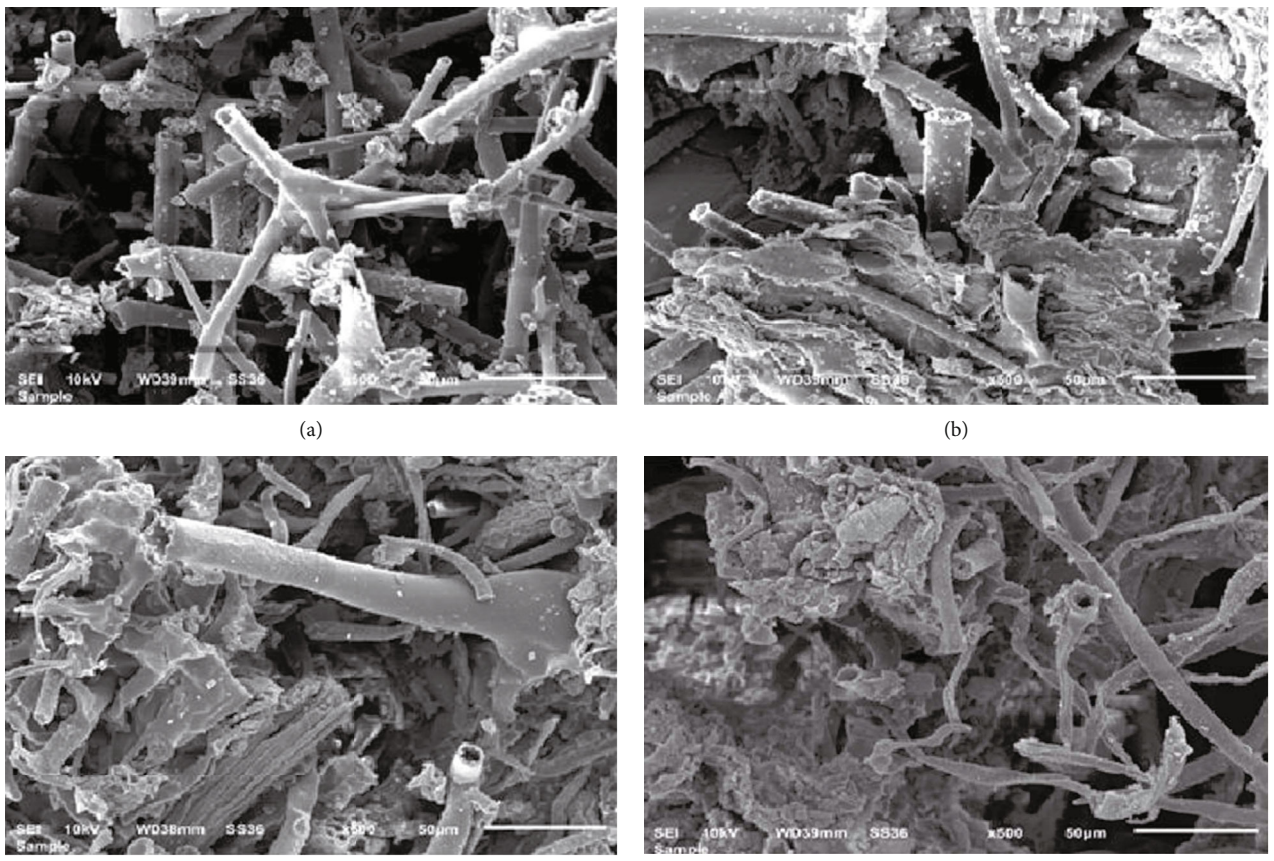

Figure 1: SEM images of TPLLP (a), Ox-TPLLP (b), Zn-TPLLP (c), and Zn/Cu-TPLLP (d).

Moreover, the values of R_L (parameter of equilibrium) related to the fundamental characteristics of the Langmuir model were computed by applying Equation (4).

$$R_L = \frac{1}{1 + K_L C_o}, \tag{4}$$

where KL is the Langmuir constant and Co is the highest CR initial concentration.

2.4.5. Thermodynamic Studies. The thermodynamic constants (ΔH°, ΔS°, and ΔG°) were assessed from the outcomes of Section 2.3 for adsorption of 100, 150, 200, 300, and 500 mg.L^{-1} CR solutions based on Equations (5) and (6).

$$\ln\left(\frac{q_e}{C_e}\right) = \frac{\Delta H^\circ}{RT} + \frac{\Delta S^\circ}{R}, \tag{5}$$

$$\Delta G^\circ = \Delta H^\circ - T\Delta S^\circ, \tag{6}$$

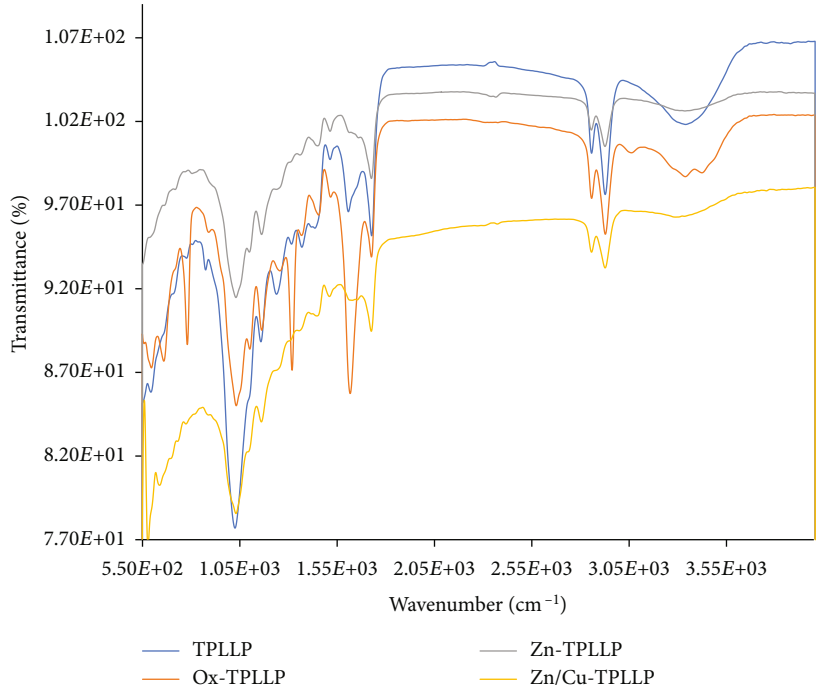

Figure 2: Spectra of FT-IR for TPLLP, Ox-TPLLP, Zn-TPLLP, and Zn/Cu-TPLLP.

where ΔH° is the enthalpy change, ΔS° is the entropy change, ΔG° is the change in standard free energy, T is the temperature of adsorption (K), and R is the universal constant of gases (8.314 J/K mol).

3. Results and Discussion

3.1. Adsorbent Characterization. Figures 1(a)–1(d) are the SEM images for adsorbent samples labeled as TPLLP, Ox-TPLLP, Zn-TPLLP, and Zn/Cu-TPLLP, respectively. In comparison between the image of an unmodified adsorbent (a) and images of the other three modified samples (b), (c), and (d), it can be detected that the surface of TPLLP is significantly changed due to the modification process, where most of folds in the modified adsorbent were collapsed and their structures became distracted. Moreover, the surfaces of the modified adsorbents contain many heterogeneous holes and pores which are supportive to the adsorption phenomena. Figure 1 also reveals that the density of the micropores on the adsorbent surface modified by $ZnCl_2$ and CuS (Zn/Cu-TPLLP) is higher than that of the other three adsorbents.

The spectra of FT-IR for unmodified and modified TPLLP are demonstrated in Figures 2. This figure reveals that the unmodified sample of TPLLP has seven peaks at 3335.93 cm^{-1} for stretching the hydrogen banded of O–H, 2923.91 cm^{-1} for C–H alkyl stretching, 2854.17 cm^{-1} for stretching of C–H, 1727.26 cm^{-1} for C=O stretching (aliphatic aldehydes), 1513.56 cm^{-1} for N-H (2°-amide) II band, 1158.35 cm^{-1} for stretching of C–O, and 1025.46 cm^{-1} for bending of C–H in-plane. Similar peaks with small shifting can be detected in the case of Zn-TPLLP and Zn/Cu-TPLLP samples (Figure 2). Figure 2 also demonstrates that three new peaks appeared in the case of Ox-TPLLP at 1616.92, 1318.54, and 780.67 cm^{-1}. The presence of these various functional groups on the surface of these adsorbents implies the chemical activity of these adsorbents.

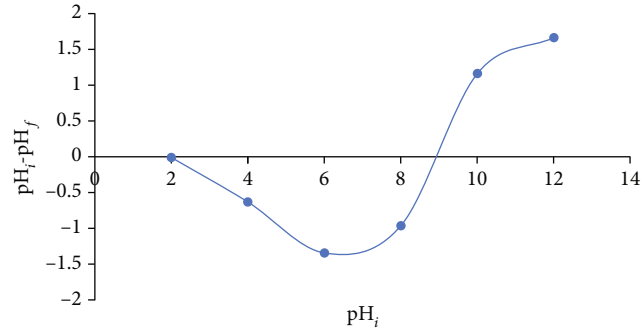

Figure 3: pH_{ZPC} of the adsorbent of Zn/Cu-TPLLP.

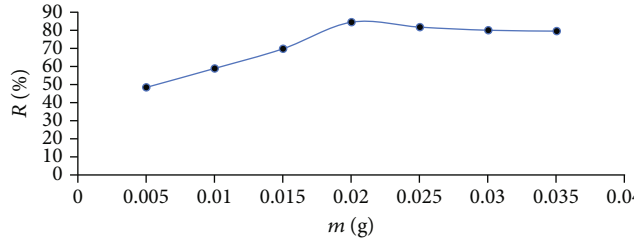

Figure 4: Influence of Zn/Cu-TPLLP dose on Congo red adsorption capacity.

According to the results of the BET surface analyzer (0.3806 $m^2.g^{-1}$, 0.001467 $cm^3.g^{-1}$, 151.065 Å), (0.7680 $m^2.g^{-1}$, 0.006674 $cm^3.g^{-1}$, 157.279 Å), (1.5875 $m^2.g^{-1}$, 0.007757 $cm^3.g^{-1}$, 400.197 Å), and (2.6436 $m^2.g^{-1}$, 0.013317 $cm^3.g^{-1}$,

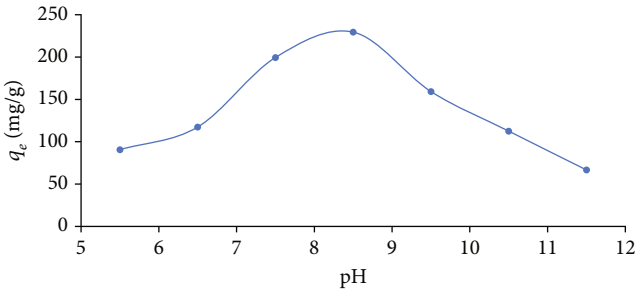

Figure 5: Influence of pH solution on Congo red adsorption by Zn/Cu-TPLLP (temperature = 27°C, C_o = 300 mg.L^{-1}, m = 0.02 g, and time = 22 h).

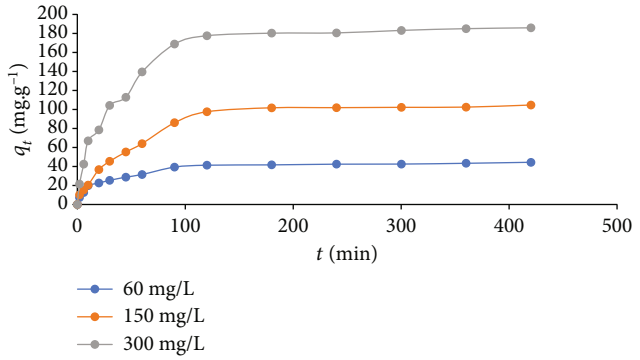

Figure 6: Influence of contact time on Congo red adsorption by Zn/Cu-TPLLP (temperature = 27°C, C_o = 60, 150, and 300 mg.L^{-1}, m = 0.02 g, and time = 0 – 420 min).

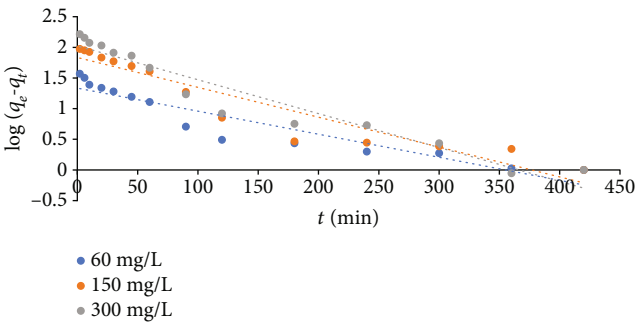

Figure 7: Kinetic model of the 1st order for Congo red adsorption by Zn/Cu-TPLLP (temperature = 27°C, C_o = 60, 150, and 300 mg.L^{-1}, m = 0.02 g, and time = 0 – 420 min).

527.393 Å) are the surface area, pore volume, and pore size of TPLLP, Ox-TPLLP, Zn-TPLLP, and Zn/Cu-TPLLP, respectively. This means that the surface area and pore characteristics of TPLLP < Ox – TPLLP < Zn – TPLLP < Zn/Cu – TPLLP. This confirms that the hydrothermal modification of TPLLP by $ZnCl_2$ and CuS has an effective role in the improvement of the porosity and surface area of this raw material.

Figure 3 depicts the relationship between the values of p H_i and (pH_i – pH_f). The pH solution value at which the surface of this ideal adsorbent will be neutrally charged is 8.8.

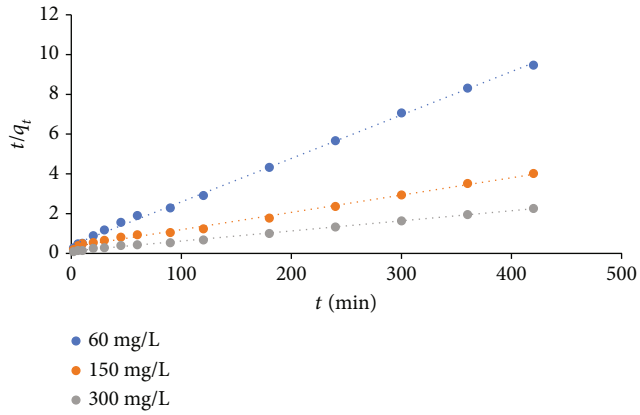

Figure 8: Kinetic model of the 2nd order for Congo red adsorption by Zn/Cu-TPLLP (temperature = 27°C, C_o = 60, 150, and 300 mg.L^{-1}, m = 0.02 g, and time = 0 – 420 min).

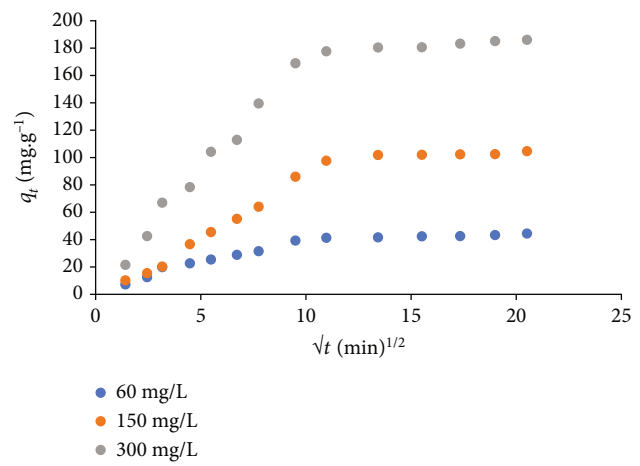

Figure 9: Model of intraparticle diffusion for Congo red adsorption by Zn/Cu-TPLLP (temperature = 27°C, C_o = 60, 150, and 300 mg.L^{-1}, m = 0.02 g, and time = 0 – 420 min).

3.2. Results of Adsorption Experiments

3.2.1. Adsorbent Performance. The percentage removal of CR from aqueous solutions by TPLLP, Ox-TPLLP, Zn-TPLLP, and Zn/Cu-TPLLP adsorbents was determined to be 17.87, 45.11, 54.94, and 78.75 percent, respectively. Moreover, the values of 11.91, 30.08, 45.06, and 52.50 (mg.g^{-1}) are the amounts of CR adsorbed at equilibrium (q_e) by these adsorbents and the same order. These values prove that the effectiveness of these adsorbents for the removing of CR is as follows:

$$\text{TPLLP} < \text{Ox} - \text{TPLLP} < \text{Zn} - \text{TPLLP} < \text{Zn/Cu} - \text{TPLLP} \quad (7)$$

This can be explained by the surface areas and pore characteristics of these adsorbents which are augmented in the same order (Section 3.1). The outcomes of this section confirm that Zn/Cu-TPLLP is the ideal sample that can be

Table 4: Parameters of the 1st- and 2nd-order kinetic models for adsorption of Congo red by Zn/CuS-TPLLP.

C_o (mg.L^{-1})	$q_{e,exp}$ (mg.g^{-1})	Kinetic model						
		1st order			2nd order			
		$q_{e1,cal}$ (mg.g^{-1})	K_1 (h^{-1})	R^2	$q_{e2,cal}$ (mg.g^{-1})	K_2 (g.mg^{-1}.h^{-1})	R^2	Rate
60	44.35	21.63	0.009	0.884	45.87	0.001167	0.999	0.054
150	104.50	68.33	0.011	0.903	114.94	0.000233	0.995	0.027
300	185.59	105.66	0.013	0.934	196.08	0.000230	0.998	0.045

applied for CR adsorption. Thus, the other experiments of this work were conducted by using Zn/Cu-TPLLP only.

3.2.2. Influence of Zn/Cu-TPLLP Dose. To define the optimal mass of Zn/Cu-TPLLP that will be required for the adsorption of CR dye and to examine the dosage influence, the values of the % removal of CR from its solutions were plotted against Zn/Cu-TPLLP doses (Figure 4). This figure shows augmenting the values of CR %R with increasing the mass of Zn/Cu-TPLLP in the range of (0.005-0.02 g). This increment was resulted from increasing the active sites of the adsorbent which are directly proportional with the amount of an adsorbent [35]. Figure 4 also displays that there is no significant change in the value of %R when the adsorbent mass increased from 0.02 g to 0.035 g because the adsorbent molecules in the case of their high doses will be assembled together to form a cluster [36]. For this, 0.02 g of Zn/Cu-TPLLP was selected as the ideal dose in this work. Similar trends were reported for the adsorption of MnO_4^- on CuS surface [37].

3.2.3. Impact of pH. The process of adsorption is strongly affected by the solution pH of the adsorbate, as the adsorbent charge and ionization degree of the dye molecules depend on the value of pH. For this reason, the influence of this factor was considered in this work (Figure 5). As indicated in Figure 5, q_e (mg.g^{-1}) was positively affected when pH elevated from 5.5 to 8.5. This was due to the strong attraction between the anions of CR ($pK_a = 4$) and the positive charges on the surface of Zn/Cu-TPLLP ($pH_{ZPC} = 8.8$). On the contrary, q_e (mg.g^{-1}) was negatively influenced by increasing pH value over 8.5 as a result of the strong repulsion between the negative ions of CR and the negative charges of this adsorbent. Similar outcomes were reported for the adsorption of CR on the surface of some solid wastes [3].

3.2.4. Kinetic Studies. Figure 6 illustrates the contact time impact on the adsorption of CR solution (60, 150, and 300 mg/L) by a fixed mass of Zn/Cu-TPLLP (0.02 g). According to this figure, there are three different adsorption stages, where the adsorption amount rapidly increased in the 1st stage (0-10 min), gradually increased in the 2nd stage (10-120 min), and almost was constant after 120 min (3rd stage). This proves that most of the sites were vacant at the first stage of this adsorption, and then, CR molecules gradually accumulated on these sites till fully occupied. The same outcomes were observed for CR adsorption by tea waste [29]. Although Figure 6 demonstrates that the equilibrium of this adsorption was achieved in 2 h, other experiments were performed at 22

Table 5: Parameters of the intraparticle-diffusion kinetic model for adsorption of Congo red by Zn/CuS-TPLLP.

C_o (mg.L^{-1})	First region			Second region		
	K_{dif} (mg/h$^{1/2}$g)	C	R^2	K_{dif} (mg/h$^{1/2}$g)	C	R^2
60	3.654	4.692	0.965	0.304	37.661	0.918
150	9.409	-6.492	0.992	0.584	92.176	0.807
300	17.613	1.601	0.987	0.881	167.580	0.971

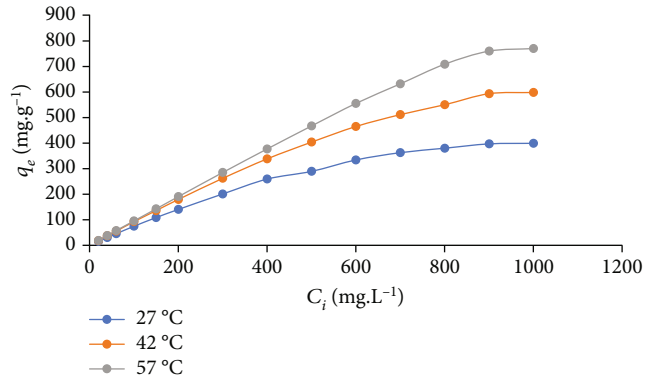

Figure 10: Influences of initial concentration and temperature on the adsorption of Congo red by Zn/Cu-TPLLP (temperature = 27, 42.57°C , C_o = 20 – 1000 mg.L^{-1}, m = 0.02 g, and time = 22 h).

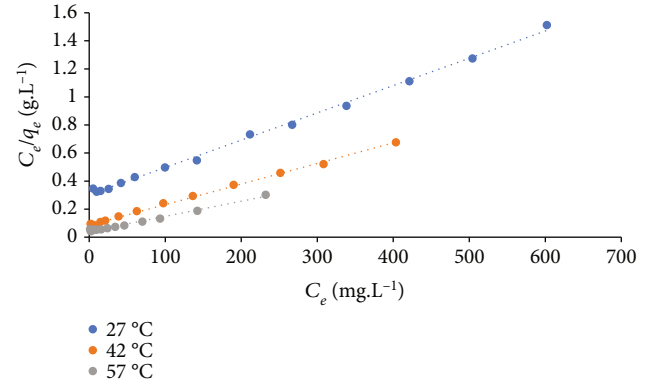

Figure 11: Langmuir isotherm for adsorption of Congo red on Zn/Cu-TPLLP (temperature = 27, 42.57°C, C_o = 20 – 1000 mg.L^{-1}, m = 0.02 g, and time = 22 h).

h to ensure that all adsorption constants have been essentially studied at equilibrium.

Moreover, the slopes and intercepts of the plots of Figure 7 (kinetic model of the 1st order), Figure 8 (kinetic model of the 2nd order), and Figure 9 (kinetic model of intraparticle diffusion) were applied for computing the dynamic parameters of this adsorption. The calculated values were recorded in Table 4 for the first- and second-order models and in Table 5 for intraparticle diffusion model. In comparison between the parameter values of the first- and second-order models (Table 4), it can be seen that R^2 (correlation coefficient) values of the first order are less than those of the second order and the empirical values of q_e ($q_{e,\ \exp}$) are significantly similar to the values of q_e calculated from the slopes of the second-order plots ($q_{e2,\ \text{cal}}$). These outcomes prove that the kinetic model of the pseudo 2nd order can be applied for describing the kinetic empirical data for this adsorption. This confirms that this adsorption occurred due to the chemical interactions between the functional groups of Zn/Cu-TPLLP and molecules of CR [38]. The same outcomes were observed for CR adsorption by conjugates of sodium alginate-*Chlorella* polypyrrole-*Chlorella*[30]

Figure 9 reveals that each one of these plots is not linear for the total interval of time; none passed from the origin point and has two linear parts which have significant values of R^2. These results are evidence that the rate of this adsorption is controlled by intraparticle diffusion and other mechanisms [39]. Furthermore, the small values of C constant (Table 5), which are associated with the adsorbent layer thickness, prove that the external diffusion of CR molecules has a negligible role in the controlling of this adsorption rate [40]. Similar trends were noted for methylene blue adsorption by $ZnCl_2$-modified Neem [41] and Lamiaceae [42].

3.2.5. Outcomes of Isotherms. The results associated with the influences of solution temperature and concentration on the performance of this adsorption are represented in Figure 10. The plots of this figure show that the adsorption of CR by Zn/Cu-TPLLP was positively influenced by the solution temperature because the CR solution viscosity and the movement energy of CR molecules decrease and increase, respectively, with rising temperature [43]. Figure 10 also shows that the values of q_e at each temperature were regularly augmented by increasing the CR concentration from 20 to 800 mg.L^{-1}. This can be explained by the fact that increasing the concentration of adsorbate will improve the force of dynamics that reduces the resistance of the mass movement of CR molecules between the adsorbate solution and the adsorbent surface [44]. Moreover, there is no variation in the values of q_e that can be seen when CR concentration increased above 800 mg.L^{-1} because all adsorption sites become full at this high concentration.

Furthermore, the analyzed experimental data of the isotherms of this adsorption are presented in Figure 11 (Langmuir model), Figure 12 (Freundlich model), and Figure 13 (Temkin model). Intercepts and slopes of the plots of these figures were used for calculation of the values of the isotherm factors recorded in Table 6. Langmuir model has the highest

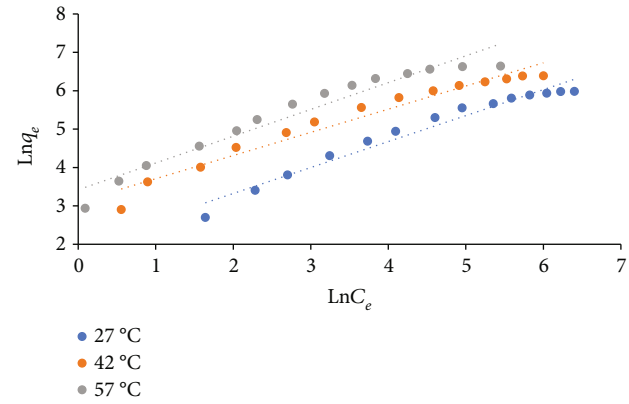

Figure 12: Freundlich isotherm for adsorption of Congo red on Zn/Cu-TPLLP (temperature = 27, 42.57°C, C_o = 20 – 1000 mg.L^{-1}, m = 0.02 g, and time = 22 h).

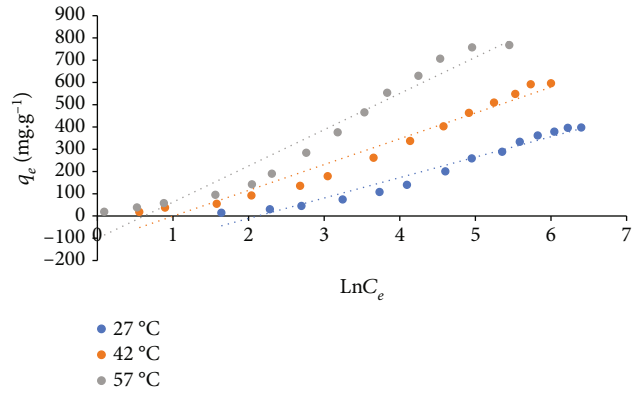

Figure 13: Temkin isotherm for adsorption of Congo red on Zn/Cu-TPLLP (temperature = 27, 42.57°C, C_o = 20 – 1000 mg.L^{-1}, m = 0.02 g, and time = 22 h).

value of R^2 compared to the other two models (Table 6), which confirms that the empirical data of this adsorption are better to be described by Langmuir model. According to these outcomes, it can be suggested that this adsorption is a monolayer and the adsorption sites of Zn/Cu-TPLLP are homogeneous [45]. Additionally, all values of R_L (dimensionless adsorption factor) and $1/n$ (Table 6) are less than unity, which confirms that the empirical conditions used in this adsorption were suitable [46]. Similar outcomes were reported for the adsorption of CR on the surface of some solid wastes [3] and hydrothermal-treated shiitake mushroom [1].

Moreover, high adsorption capacities of 526.32, 666.67, and 909.09 (mg.g^{-1}) (Table 6) were obtained at the temperatures of 27, 42, and 57°C, respectively. This proves that Zn/Cu-TPLLP as a cheap and effective adsorbent will meet special interesting in the purification processes of wastewaters and water from CR.

3.2.6. Thermodynamic Outcomes. The values of ln (q_e/C_e) for adsorption of 100, 150, 200, 300, and 500 (mg.L^{-1}) CR solutions by 0.02 g of Zn/Cu-TPLLP were calculated and plotted vis. T^{-1} (K^{-1}) (Equation (5)) (Figure not shown). Slopes and

Table 6: Isotherm constants for adsorption of Congo red by Zn/CuS-TPLLP.

Temperature	Isotherm parameters										
	Langmuir				Freundlich				Temkin		
	q_{max} (mg.g^{-1})	K_L (L.mg^{-1})	R_L	R^2	K_F (mg.g^{-1}) (L.mg^{-1})$^{1/n}$	$1/n$	n	R^2	K_T (L.mg^{-1})	B_1	R^2
27°C	526.32	0.0063	0.137	0.997	7.174	0.676	1.479	0.965	0.120	91.81	0.963
42°C	666.67	0.0176	0.054	0.997	22.294	0.604	1.656	0.957	0.366	115.89	0.965
57°C	909.09	0.0270	0.036	0.990	30.560	0.698	1.433	0.944	0.539	162.73	0.952

Table 7: Thermodynamic constants for adsorption of Congo red by Zn/CuS-TPLLP.

Initial concentration (mg.L^{-1})	ΔH° (kJ.mol^{-1})	ΔS° (kJ.mol^{-1})	ΔG° (kJ.mol^{-1})			R^2
			300 K	315 K	330 K	
100	53.299	0.1876	-2.9847	-5.7989	-8.6131	0.944
150	54.046	0.1887	-2.5699	-5.4007	-8.2314	0.980
200	57.560	0.1994	-2.2706	-5.2621	-8.2536	0.988
300	60.070	0.2062	-1.7958	-4.8891	-7.9824	0.999
500	63.024	0.2124	-0.7000	-3.8863	-7.0725	0.998

Table 8: Adsorbents used for adsorption of Congo red.

Adsorbents	Q max (mg.g^{-1})	Temperature	Sources
Zn/Cu-TPLLP	526.3	27°C	This work
	666.7	42°C	
	909.1	57°C	
Treated shrimp shell particle (TSSP)	232.0	30°C	[2]
	264.6	40°C	
	288.2	50°C	
Raw shrimp shell particle (RSSP)	182.1	30°C	[2]
	234.7	40°C	
	256.4	50°C	
Bottom ash	1.1		[3]
Deoiled soya	1.1		[3]
Montmorillonite	714.3		[21]
Hydrothermal-treated shiitake mushroom	217.9	20°C	[1]
	211.9	35°C	
	209.4	50°C	
Tea waste	32.3		[29]
Conjugates of sodium alginate-*Chlorella* polypyrrole-*Chlorella*	772.7	30°C	[30]

intercepts of the resulted curves were used for evaluating the ΔH° and ΔS° values, respectively. Then, the values of ΔG° at each temperature were calculated from the obtained values of ΔS° and ΔH° based on Equation (6). The calculated values of these parameters (ΔG°, ΔS°, and ΔH°) are listed in Table 7. The ΔG° negative values imply that the adsorption of CR by Zn/Cu-TPLLP in the range of 300-330 K is spontaneous [2]. Endothermic adsorption of CR by this adsorbent can be confirmed by the positive ΔH°[46], which is agreed well with the outcomes of Section 3.2.5 (effect of temperature part). Additionally, ΔH° values are in the range of 53.229-63.024 kJ.mol^{-1} (higher than 20.9 kJ.mol^{-1}), implying that CR was chemically adsorbed on the surface of Zn/Cu-TPLLP [47]. This is in consistent with the kinetic part results. Furthermore, ΔS° and ΔH° positive values prove that the force of driving for this adsorption is effected by ΔS° rather ΔH°[48].

3.3. Comparison with Other Low-Cost Adsorbents. The capacities of CR adsorption by Zn/Cu-TPLLP and other common low-cost adsorbents are given in Table 8. As shown, Zn/Cu-TPLLP, due to its significant chemical activity, has adsorption capacity higher than those of the common low-cost adsorbents used for removal of CR from the aqueous solutions before this work. Thus, the low cost of Zn/Cu-TPLLP

is along with its higher adsorptive performance which confirms the importance and novelty of this adsorbent among the other low-cost adsorbents previously used for removing of CR from wastewaters.

4. Conclusions

In this research, the leaf powder of *Teucrium polium L.* (TPLLP) was modified by oxalic acid, CuS, and $ZnCl_2$. The modified and unmodified samples were characterized and tested for adsorption of Congo red (CR). The sample modified by the mixture of CuS and $ZnCl_2$ (Zn/Cu-TPLLP) was the best (%$R = 78.75$) among these four adsorbents. Thus, Zn/Cu-TPLLP was selected in this work as a novel adsorbent for adsorption of CR dye from the aqueous solutions. The surface area, pore volume, pore size, and pH_{ZPC} of Zn/Cu-TPLLP were found to be 2.6436 $m^2.g^{-1}$, 0.013317$cm^3.g^{-1}$, 527.393 Å, and 8.8, respectively. Impacts of temperature, pH, concentration of CR solution, dosage of Zn/Cu-TPLLP, and contact time on this adsorption were studied. It was noted that this adsorption is positively affected when temperature, pH, adsorbent dose, CR concentration, and time of contact were augmented in the ranges of 27-57°C, 5.5-8.5, 0.005-0.02 g, 20-900 $mg.L^{-1}$, and 0-120 min, respectively. The capacities of this adsorption almost were equal when CR concentration, Zn/Cu-TPLLP dosage, and time of adsorption were increased over 900 $mg.L^{-1}$, 0.02 g, and 120 min, correspondingly. Additionally, it was found that this adsorption negatively influenced when pH increased in the range of 8.5-11. Kinetic and isotherm results proved that this adsorption was described well by the kinetic model of the 2nd order and the isotherm model of Langmuir. Kinetic and thermodynamic outcomes confirmed the chemisorption nature of CR by Zn/Cu-TPLLP. Spontaneous and endothermic properties of this adsorption were proved by the results of thermodynamic. The high capacities of this adsorption (526.32, 666.67, and 909.09 $mg.g^{-1}$) imply that Zn/Cu-TPLLP will meet special interesting in the field of polluted water treatment among the other low-cost adsorbents.

Data Availability

Completely, data produced or investigated during this work were involved in this submitted article.

Conflicts of Interest

The authors confirmed that there are no probable conflicts of interest that impact the work reported in this paper.

Acknowledgments

The authors are very appreciative to the Deanship of Scientific Research at Tabuk University for funding the work through new faculty research/funding (Project No. S-0095-1441H).

References

[1] K. Yang, Y. Li, H. Zheng et al., "Adsorption of Congo red with hydrothermal treated shiitake mushroom," *Materials Research Express*, vol. 7, article 015103, 2020.

[2] Y. Zhou, L. Ge, N. Fan, and M. Xia, "Adsorption of Congo red from aqueous solution onto shrimp shell powder," *Adsorption Science & Technology*, vol. 36, no. 5-6, pp. 1310–1330, 2018.

[3] A. Mittal, J. Mittal, A. Malviya, and V. K. Gupta, "Adsorptive removal of hazardous anionic dye "Congo red" from wastewater using waste materials and recovery by desorption," *Journal of Colloid and Interface Science*, vol. 340, no. 1, pp. 16–26, 2009.

[4] Q. du, J. Sun, Y. Li et al., "Highly enhanced adsorption of Congo red onto graphene oxide/chitosan fibers by wet-chemical etching off silica nanoparticles," *Chemical Engineering Journal*, vol. 245, pp. 99–106, 2014.

[5] A. R. Binupriya, M. Sathishkumar, K. Swaminathan, C. S. Kuz, and S. E. Yun, "Comparative studies on removal of Congo red by native and modified mycelial pellets of Trametes versicolor in various reactor modes," *Bioresource Technology*, vol. 99, no. 5, pp. 1080–1088, 2008.

[6] A. Afkhami and R. Moosavi, "Adsorptive removal of Congo red, a carcinogenic textile dye, from aqueous solutions by maghemite nanoparticles," *Journal of Hazardous Materials*, vol. 174, no. 1-3, pp. 398–403, 2010.

[7] S. Chakraborty, B. Basak, S. Dutta, B. Bhunia, and A. Dey, "Decolorization and biodegradation of Congo red dye by a novel white rot fungus Alternaria alternata CMERI F6," *Bioresource Technology*, vol. 147, pp. 662–666, 2013.

[8] R. K. Sonwani, G. Swain, B. S. Giri, R. S. Singh, and B. N. Rai, "Biodegradation of Congo red dye in a moving bed biofilm reactor: performance evaluation and kinetic modeling," *Bioresource Technology*, vol. 302, p. 122811, 2020.

[9] Z. Y. Velkova, G. K. Kirova, M. S. Stoytcheva, and V. K. Gochev, "Biosorption of Congo red and methylene blue by pretreated waste Streptomyces fradiae biomass – equilibrium, kinetic and thermodynamic studies," *Journal of the Serbian Chemical Society*, vol. 83, no. 1, pp. 107–120, 2018.

[10] A. Akhtar, Z. Aslam, A. Asghar, M. M. Bello, and A. A. A. Raman, "Electrocoagulation of Congo red dye-containing wastewater: optimization of operational parameters and process mechanism," *Journal of Environmental Chemical Engineering*, vol. 8, no. 5, p. 104055, 2020.

[11] H. Kristianto, M. Y. Tanuarto, S. Prasetyo, and A. K. Sugih, "Magnetically assisted coagulation using iron oxide nanoparticles-Leucaena leucocephala seeds' extract to treat synthetic Congo red wastewater," *International Journal of Environmental Science and Technology*, vol. 17, no. 7, pp. 3561–3570, 2020.

[12] T. Hou, K. Guo, Z. Wang et al., "Glutaraldehyde and polyvinyl alcohol crosslinked cellulose membranes for efficient methyl orange and Congo red removal," *Cellulose*, vol. 26, no. 8, pp. 5065–5074, 2019.

[13] Z. Mao-Xu, L. Li, W. Hai-Hua, and W. Zheng, "Removal of an anionic dye by adsorption/precipitation processes using alkaline white mud," *Journal of Hazardous Materials*, vol. 149, pp. 735–741, 2007.

[14] S. Argote-Fuentes, R. Feria-Reyes, E. Ramos-Ramírez, N. Gutiérrez-Ortega, and G. Cruz-Jiménez, "Photoelectrocatalytic degradation of Congo red dye with activated hydrotalcites and copper anode," *Catalysts*, vol. 11, no. 2, p. 211, 2021.

[15] N. Ali, A. Said, F. Ali et al., "Photocatalytic degradation of Congo red dye from aqueous environment using cobalt ferrite nanostructures: development, characterization, and photocatalytic performance," *Water, Air, and Soil Pollution*, vol. 231, no. 2, p. 50, 2020.

[16] S. A. Bhat, F. Zafar, A. H. Mondal et al., "Photocatalytic degradation of carcinogenic Congo red dye in aqueous solution, antioxidant activity and bactericidal effect of NiO nanoparticles," *Journal of the Iranian Chemical Society.*, vol. 17, no. 1, pp. 215–227, 2020.

[17] Y. P. Bhoi, S. R. Pradhan, C. Behera, and B. G. Mishra, "Visible light driven efficient photocatalytic degradation of Congo red dye catalyzed by hierarchical CuS–Bi2CuxW1−xO6−2xnanocomposite system," *RSC Advances*, vol. 6, no. 42, pp. 35589–35601, 2016.

[18] J. Fowsiya, G. Madhumitha, N. A. Al-Dhabi, and M. V. Arasu, "Photocatalytic degradation of Congo red using Carissa edulis extract capped zinc oxide nanoparticles," *Journal of Photochemistry and Photobiology B: Biology*, vol. 162, pp. 395–401, 2016.

[19] P. M. O. Ikhazuangbe, K. K. Adama, and G. I. Akintoye, "Adsorption of Congo red dye onto activated carbon from periwinkle shell," *Nigerian Journal of Engineering Science Research*, vol. 3, pp. 63–75, 2020.

[20] R. Lafi, I. Montasser, and A. Hafiane, "Adsorption of Congo red dye from aqueous solutions by prepared activated carbon with oxygen-containing functional groups and its regeneration," *Adsorption Science & Technology*, vol. 37, no. 1-2, pp. 160–181, 2019.

[21] Y. O. Khaniabadi, M. J. Mohammadi, M. Shegerd, S. Sadeghi, S. Saeedi, and H. Basiri, "Removal of Congo red dye from aqueous solutions by a low-cost adsorbent: activated carbon prepared from aloe vera leaves shell," *Environmental Health Engineering and Management Journal*, vol. 4, pp. 29–35, 2017.

[22] A. Kausar, M. Iqbal, A. Javed et al., "Dyes adsorption using clay and modified clay: a review," *Journal of Molecular Liquids*, vol. 256, pp. 395–407, 2018.

[23] S. Zhang, L. Zhong, H. Yang, A. Tang, and X. Zuo, "Magnetic carbon-coated palygorskite loaded with cobalt nanoparticles for Congo red removal from waters," *Applied Clay Science*, vol. 198, p. 105856, 2020.

[24] S. Z. Mohammadi, Z. Safari, and N. Madady, "Synthesis of Co3O4@SiO2 core/shell–nylon 6 magnetic nanocomposite as an adsorbent for removal of Congo red from wastewater," *Journal of Inorganic and Organometallic Polymers and Materials*, vol. 30, no. 8, pp. 3199–3212, 2020.

[25] J. Mohanta, S. Dey, and S. Dey, "Highly porous iron-zirconium binary oxide for efficient removal of Congo red from water," *Desalination and Water Treatment*, vol. 189, pp. 227–242, 2020.

[26] B. Priyadarshini, T. Patra, and T. R. Sahoo, "An efficient and comparative adsorption of Congo red and trypan blue dyes on MgO nanoparticles: kinetics, thermodynamics and isotherm studies," *Journal of Magnesium and Alloys*, vol. 16, p. 53, 2021.

[27] E. Abdelkader, L. Nadjia, and V. Rose-Noelle, "Adsorption of Congo red azo dye on nanosized SnO2 derived from sol-gel method," *International Journal of Industrial Chemistry*, vol. 7, no. 1, pp. 53–70, 2016.

[28] L. Bulgariu, L. B. Escudero, O. S. Bello et al., "The utilization of leaf-based adsorbents for dyes removal: a review," *Journal of Molecular Liquids*, vol. 276, pp. 728–747, 2019.

[29] M. Foroughi-Dahr, H. Abolghasemi, M. Esmaili, A. Shojamoradi, and H. Fatoorehchi, "Adsorption characteristics of Congo red from aqueous solution onto tea waste," *Chemical Engineering Communications*, vol. 202, pp. 181–193, 2015.

[30] M. Maqbool, S. Sadaf, H. N. Bhatti et al., "Sodium alginate and polypyrrole composites with algal dead biomass for the adsorption of Congo red dye: kinetics, thermodynamics and desorption studies," *Surfaces and Interfaces*, vol. 25, article 101183, 2021.

[31] E. Al-Shalabi, M. Alkhaldi, and S. Sunoqrot, "Development and evaluation of polymeric nanocapsules for cirsiliol isolated from Jordanian _Teucrium polium_ L. as a potential anticancer nanomedicine," *Journal of Drug Delivery Science and Technology*, vol. 56, article 101544, 2020.

[32] M. Khazaei, S. N. Nematollahi-Mahani, T. Mokhtari, and F. Sheikhbahaei, "Review on Teucrium polium biological activities and medical characteristics against different pathologic situations," *Journal of Contemporary Medical Sciences*, vol. 4, pp. 1–6, 2018.

[33] M. A. J. Kouhbanani, N. Beheshtkhoo, S. Taghizadeh, A. M. Amani, and V. Alimardani, "One-step green synthesis and characterization of iron oxide nanoparticles using aqueous leaf extract ofTeucrium poliumand their catalytic application in dye degradation," *Advances in Natural Sciences: Nanoscience and Nanotechnology*, vol. 10, no. 1, article 015007, 2019.

[34] P. Karimi, S. Javanshir, M. H. Sayadi, and H. Arabyarmohammadi, "Arsenic removal from mining effluents using plant-mediated, green-synthesized iron nanoparticles," *PRO*, vol. 7, no. 10, p. 759, 2019.

[35] S. R. Kuchekar, P. M. Patil, B. Vishwas, H. Gaikwad, and S. Han, "Synthesis and characterization of silver nanoparticles using Azadirachta indica (Neem) leaf extract," *International Journal of Engineering Science Invention*, vol. 6, pp. 47–55, 2017.

[36] F. Nekouei, S. Nekouei, I. Tyagi, and V. K. Gupta, "Kinetic, thermodynamic and isotherm studies for acid blue 129 removal from liquids using copper oxide nanoparticle-modified activated carbon as a novel adsorbent," *Journal of Molecular Liquids*, vol. 201, pp. 124–133, 2015.

[37] M. M. H. Aljohani and H. A. al-Aoh, "Adsorptive removal of permanganate anions from synthetic wastewater using copper sulfide nanoparticles," *Materials Research Express*, vol. 8, no. 3, article 035012, 2021.

[38] W. C. Wanyonyi, J. M. Onyari, and P. M. Shiundu, "Adsorption of Congo red dye from aqueous solutions using roots of Eichhornia crassipes : kinetic and equilibrium studies," *Energy Procedia*, vol. 50, pp. 862–869, 2014.

[39] Y. S. Ho and G. McKay, "The kinetics of sorption of basic dyes from aqueous solution by sphagnum moss peat," *Canadian Journal of Chemical Engineering*, vol. 76, no. 4, pp. 822–827, 1998.

[40] J. W. Lin, Y. H. Zhan, and Z. L. Zhu, "Adsorption characteristics of copper (II) ions from aqueous solution onto humic acid-immobilized surfactant-modified zeolite," *Colloids and Surfaces A: Physicochemical and Engineering Aspects*, vol. 384, no. 1-3, pp. 9–16, 2011.

[41] S. K. Mustafa, H. A. Al-Aoh, S. A. Bani-Atta et al., "Enhance the adsorption behavior of methylene blue from waste-water by using $ZnCl_2$ modified Neem (*Azadirachta indica*) leaves powder," *Desalination and Water Treatment*, vol. 209, no. 2021, pp. 367–378, 2020.

[42] M. M. H. Aljohani, J. M. J. Almizraq, A. M. Albalawi et al., "Efficient dye discoloration of modified Lamiaceae leaves," *Materials Research Express*, vol. 8, article 035503, 2021.

[43] B. H. Hameed and A. A. Ahmad, "Batch adsorption of methylene blue from aqueous solution by garlic peel, an agricultural waste biomass," *Journal of Hazardous Materials*, vol. 164, no. 2-3, pp. 870–875, 2009.

[44] B. Qu, J. Zhou, X. Xiang, C. Zheng, H. Zhao, and X. Zhou, "Adsorption behavior of Azo Dye C. I. Acid Red 14 in aqueous solution on surface soils," *Journal of Environmental Sciences*, vol. 20, pp. 704–709, 2008.

[45] A. A. A. Darwish, M. Rashad, and H. A. Al-Aoh, "Methyl orange adsorption comparison on nanoparticles: isotherm, kinetics, and thermodynamic studies," *Dyes and Pigments*, vol. 160, pp. 563–571, 2019.

[46] M. Ceglowski and G. Schroeder, "Removal of heavy metal ions with the use of chelating polymers obtained by grafting pyridine-pyrazole ligands onto polymethylhydrosiloxane," *Chemical Engineering Journal*, vol. 259, pp. 885–893, 2015.

[47] A. Kurniawan and S. Ismadji, "Potential utilization of _Jatropha curcas L._ press-cake residue as new precursor for activated carbon preparation: Application in methylene blue removal from aqueous solution," *Journal of the Taiwan Institute of Chemical Engineers*, vol. 42, no. 5, pp. 826–836, 2011.

[48] H. J. Hou, R. H. Zhou, P. Wu, and L. Wu, "Removal of Congo red dye from aqueous solution with hydroxyapatite/chitosan composite," *Chemical Engineering Journal*, vol. 211-212, pp. 336–342, 2012.